Colloids and Surfaces B: Biointerfaces 165 (2018) 28–36

Contents lists available at ScienceDirect

Colloids and Surfaces B: Biointerfaces

journal homepage: www.elsevier.com/locate/colsurfb

A simple approach for fabrication of optical affinity-based bioanalytical microsystem on polymeric PEN foils

Alena Semerádtová[a], Marcel Štofik[a,*], Oldřich Neděla[b], Ondřej Staněk[c], Petr Slepička[b], Zdeňka Kolská[a], Jan Malý[a]

[a] Department of Biology and Material Centre, Faculty of Science, University of J.E. Purkinje, 400 96 Ústí nad Labem, Czech Republic
[b] Department of Solid State Engineering, University of Chemistry and Technology, 166 28 Prague, Czech Republic
[c] Institute of Microbiology of the CAS, v. v. i., 142 20, Praha 4, Czech Republic

ARTICLE INFO

Article history:
Received 2 November 2017
Received in revised form 23 January 2018
Accepted 24 January 2018
Available online 2 February 2018

Keywords:
Polyethylene naphthalate (PEN)
Laser micropatterning
Contact mask
Affinity-based assay
Optical biosensor
Human serum albumin (HSA)

ABSTRACT

Herein, we report a novel concept of low-cost flexible platform for fluorescence-based biosensor. The surface of polyethylene naphthalate (PEN) foil was exposed to KrF excimer laser through a photolithographic contact mask. Laser initiated surface modification resulted in micro-patterned areas with surface functional groups available for localized covalent immobilization of biotin. High affinity binding protein (albumin-binding domain (ABD) of protein G, *Streptococcus* G148) recognizing human serum albumin (HSA), genetically fused with streptavidin (SA-ABDwt), was immobilized on the micro-patterned surface through biotin-streptavidin coupling. Fluorescently labelled HSA analyte was detected in several blocking environments, in 1% bovine serum albumin (BSA) and 6% fetal serum albumin (FBS), respectively. We conclude that the presented novel concept enabled us to micropattern functional biosensing layers on the surface of PEN foil in a fast and easy way. It brings all necessary aspects for continuous roll-to-roll fabrication of low-cost optical bioanalytical devices.

1. Introduction

Optical sensing strategies include numerous approaches and can be applied in many fields such as medicine, pharmaceuticals, toxicology, environmental monitoring and others [1]. In clinical diagnostics, proteins are one of the most frequently detected components in body fluids [2]. For their optical detection, label-based immunoassays, which can also be classified as optical biosensors [3], are used as the most common qualitative and quantitative detection methods [4]. Singleplex formats (detection of single target molecules in analyte) of affinity-based immunoassays such as ELISAs (Enzyme-Linked Immunosorbent Assays) [5] have been the basic diagnostic systems for a long period of time. Recent progress in the development of fabrication techniques in microtechnology has facilitated the miniaturization of the immunoassays. These miniaturized analytical systems, the so-called protein microchips or microarrays, have not only been used as singleplex but also as multiplex detection formats (detection of multiple target molecules in analyte) [6]. Their basic components are micropatterns, often designed as microspots, with immobilized recognition elements. They provide affinity-based optical analysis of the measured samples and their main advantages, in comparison with macrosystems, are: i) increased sensitivity, described and explained by Ekins in 1990s [7], ii) multiplex samples detection in one experiment and iii) low consumption of the analysed samples. Progress in the miniaturization also facilitated the development of microfluidic immunoassays and their integration into more complex Lab-on-Chip microdevices [8].

The crucial factor in the development of robust immunoassays is the quality of the immobilization process preserving important affinity-based properties of the immobilized proteins. If proper orientation of the proteins on the immobilization surface is necessary, a bioaffinity method performed with avidin-biotin system can be considered a suitable strategy [9].

Because immobilization is usually performed on solid surfaces, their chemical and physical properties are important for the overall performance of the detection system. From the fabrication point of view, immobilization techniques for generation of micropatterns on 2D surfaces have been intensively studied in the last decades. Several different types of contact and non-contact techniques have been developed [10] and some of them can be performed in a high throughput automatized arrangement. As the most com-

* Corresponding author.
E-mail address: marcel.stofik@ujep.cz (M. Štofik).

https://doi.org/10.1016/j.colsurfb.2018.01.048
0927-7765/

monly used substrates, onto which immobilization is performed, are glass, silicon, thin metal films, polymers such as polystyrene (PS), polycarbonate (PC), polymethylmethacrylate (PMMS), cyclic olefin copolymers (COC), 3D matrixes such as hydrogels, nylon or nitrocellulose and others, reviewed in [11].

Recently, thin and flexible polymeric materials have been used for the development of Lab-on-a-Chip systems, the so-called Lab-on-a-Foil [12]. These polymeric foils become materials for fabrication of MEMS sensoric devices [13], and in life science applications for simple or more complex microfluidic solutions [14], filtration and separation devices for molecules [15], biosensors [16] or flexible electrode arrays [17]. Due to their relatively straightforward physical or chemical modification [18], natural flexibility, easy way of micro- or nano-structuring, and their potential to be processed by hot embossing [19] necessary for the device mass-production, polymeric foils are good candidate materials for a low-cost and a high-volume production of commercial microsystems. Moreover, their specific modifications by roll-to-roll processing enable effective immobilization of bioaffinity molecules in manufactured microdevices [20].

Laser material processing is a widely used manufacturing technique in industrial applications [21]. It can be used for bulk material and also for material surface processing. Laser processing can also be used as a serial microfabrication technology. It has been shown that by exposing the surface of polymeric material to a focused excimer laser beam with an intensity below the ablation threshold, permanent morphological changes in the form of regular micro- to nano-patterns, laser-induced periodic surface structures (LIPSS) can be induced. Such physical changes can be performed on various polymeric substrates [22], where periodic pattern or significant roughness increase may be induced [23,24]. Moreover, polymer foil treatment with laser beam can induce chemical changes on its surface [25]. Chemical surface modification of polymer with laser beam leads to surface oxidation with a high number of available carbonyl groups. Such activated surface of polymers can be exploited in biosensing application for immobilization of various bioactive molecules to the polymer surfaces [26,27].

In this work, we present a proof of concept (PoC) of a relatively cheap, simple, high-volume and roll-to-roll production compatible fabrication process of fluorescence-based biosensor designed on excimer laser micropatterned PEN foil, which is further modified with biotin to suit avidin-biotin affinity-based immobilization of the sensing molecules. This patterned foil was integrated into a well-based format with 8 μl of working sample per well. The functionality and analytical performance of the device was verified on detection of model analyte, human serum albumin (HSA), recognized by recombinant albumin-binding domain (ABD) of protein G (*Streptococcus* G148), genetically fused with streptavidin (SA-ABDwt) and immobilized on biotinylated surface of the device [28]. Although the patterning of substrates through a photolithography mask with excimer laser for bioapplications was already published [29], to our best knowledge, a patterning process through a contact photolithography mask on a PEN foil has not been used for diagnostic affinity based systems so far. Our concept can be further developed and integrated into more sophisticated Lab-on-a-Foil systems or it can be further developed for point of care diagnostics (POCs) and as a clinical diagnostic tool.

2. Materials and methods

Biaxially oriented polyethylene naphthalate foils (1.36 g cm^{-3}, thickness of 0.05 mm, *T*m ~ 250–290 °C, *T*g ~ 120 °C) supplied by Goodfellow Ltd., UK; O-(2-Aminoethyl)-*O*′-[2-(biotinylamino)ethyl]octaethylene glycol (PEG-biotin) was supplied by Polypure, Norway, ATTO 542 NHS-ester supplied by ATTO-TEC GmbH, Germany; bovine serum albumin (BSA) – albumin Fraction V, biotin-free supplied by Carl Roth GmbH, Germany; human serum albumin (HSA), fetal serum albumin (FBS), N-(3-Dimethylaminopropyl)-N′-ethylcarbodiimide hydrochloride (EDC), ethanolamine, Hellmanex™ III, Corning® microscope slides 25 × 75 mm were supplied by Sigma–Aldrich, Czech Republic; abrasive powder (50 μm aluminium oxide, Comco Inc., USA) was supplied by Epak Electronics Ltd, United Kingdom; recombinant proteins, streptavidin coupled with ABD binding domain (SA-ABDwt), were constructed, expressed and purified in our labs; 3M™ Laminating Adhesives – 7955MPL were supplied by G3 s.r.o., Czech Republic; p.a. grade chemicals for buffers were supplied by Sigma–Aldrich, Czech Republic and prepared in deionized water.

2.1. Micropatterning of the PEN foil

Details on the micropatterning of PEN foil were already published elsewhere [26]. In brief, a photolithography mask was fabricated by electron beam lithography (VEGAII, TESCAN Brno, s.r.o., Czech Republic) with 12 testing fields. The testing fields were arranged into 3 rows and 4 columns. Every testing field contained several small squares arranged into a square. The length of the small square edge was 200 μm. PEN foil was cut to the size of a microscope glass slide. It was put on a holder and covered by a contact mask. The surface of the foil was irradiated by excimer laser beam (Lambda Physik Compex Pro 50, Coherent Inc., USA) through each designed testing field (12 fields) in a step by step process. The laser fluence was set to 8 mJ cm^{-2} with a frequency of 10 Hz, and 100, 250 or 500 pulses were applied. A scheme of the micropatterning and the biosensor fabrication process is presented in Fig. 1.

2.2. Fabrication of the biosensor

12 holes with a diameter of 3 mm were cut into a microscopy glass slide by a precise CNC microblasting lathe (Comco Inc., USA). An AccuFlo® nozzle (type MB2520-30, Comco Inc. USA) with an opening of 0.76 mm diameter was used in combination with particles of 50 μm. The holes were arranged (designed) in the same way as the micropatterned testing fields on the foil. Then, the glass slides were sonicated in 2% solution of Hellmanex™ III for 30 min. They were rinsed thoroughly by deionized water and dried by nitrogen flow. The bottom part of the glass was covered with laminating adhesive, which had been cut to fit the size of a microscopy glass. The adhesive under the holes was removed by a dissection needle. The glass slide with the adhesive was put into contact with the top (micropatterned) surface of the foil so that the micropatterned surface of the foil created the bottom of the well. The bottom part of the well (the patterned foil) was further chemically modified and used as an active detection part. In the same manner, testing wells analogical to microtitter plate (testing strip) were created above every testing field. The volume of chemicals which were further used during each step of the performed assays was 8 μl. Subsequently, the wells were incubated in the solution of EDC (100 mg/ml of EDC in MES buffer) and PEG-biotin (100 mg/ml in DMSO) in ratio 7:1 (biotin concentration in the reactive mixture was 12.5 mg/ml) at 4 °C for 90 min. After the incubation of the micropatterned foil surface with the mixture of EDC and PEG-biotin, the surface of the PEN foil was incubated in 1% ethanolamine in dH_2O for one hour to block the rest of the activated carboxyl groups on the foil surface.

2.3. Affinity-based assays

For the performed assays, streptavidin and HSA were conjugated with a fluorescent dye ATTO 542 NHS-ester (Atto-tec, Germany) according to the dye manufacturer protocols. When the biotin-streptavidin interaction was tested, the fluorescently

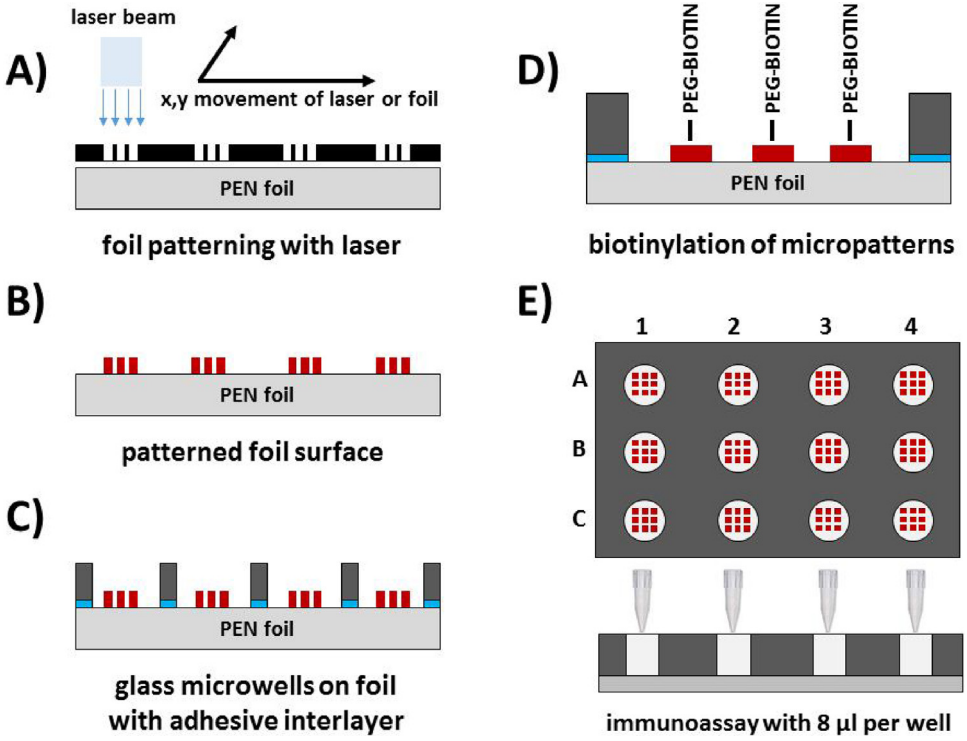

Fig. 1. Fabrication of biotinylated micropatterns.
The surface of PEN foil was exposed to laser beam through a contact mask by positioning of the laser beam above the transparent parts of the photomask in a serial manner (A). In a specified position of the laser above the mask, a certain number of laser pulses with a defined output were applied and the laser was moved to the next position. By this process, micropatterned areas were fabricated on the PEN foil (B). Then, glass slides with cut holes with laminated adhesive were put into contact with the patterned foil and a well-based format of detection system was created (C). Coupling of biotin to the micropatterned foil surface followed (D) and the biotinylated micropatterns on the PEN foil were ready for affinity-based assays (E) with 12 testing wells.

labelled streptavidin was diluted in a blocking solution of 1% BSA in 0.15 M NaCl, 0.1 M PBS, pH 7.2 (blocking buffer) and the concentration aliquots were prepared. Then, the streptavidin was pipetted into the test and the control wells and incubated at 4 °C for 30 min. All control wells had surfaces micropatterned by laser beam, but they were not biotinylated. During the assays, they were treated only with appropriate pure dilution buffers, solvents or blocking solutions. After the incubation, all wells were gently washed with deionized water and dried with nitrogen stream. In the experiments, where the amount of the immobilized biotin was optimized, we used the same protocol as described above and tested 5 different concentration ratios of PEG-biotin in an activating buffer (100 mg/ml of EDC in MES buffer) by gradual dilutions of the original solution (1:32, 1:16, 1:8, 1:4, 1:2, 1:1) resulting in concentrations of the PEG-biotin in the immobilization mixtures from 1.56 to 50.00 mg/ml. In the affinity-based assay, the concentration aliquots of SA-ABDwt (10 µg/ml) and fluorescently labelled HSA (the concentration aliquots were prepared in the scale range of 0–30 µg/ml) were prepared in a blocking solution of 1% BSA or 6% FBS (in 0.15 M NaCl, 0.1 M PBS, pH 7.2) separately. SA-ABDwt was pipetted into the test wells and incubated at 4 °C for 30 min. The control wells were incubated and washed 3 x only with the appropriate blocking solution, and HSA-ATTO 542 was pipetted into all wells. After 60 min of the incubation, all wells were gently washed with deionized water and dried with nitrogen stream.

2.4. Design and preparation of albumin binding domain-streptavidin fusion protein (SA-ABDwt)

The design and the construction of the SA-ABDwt protein was described recently [28]. Briefly, an open reading frame encoding a TRP leader-ABDwt was PCR-amplified on the templates of plasmid DNA [30] with specific primers (TabdSpeI-5′-tcactagtatgaaagcaattttcgtactg-3′ and TabdHindIII-5′-caaagcttgaaccagggatcaaggtaa-3′) and fused in a frame to the 3′ end of a codon-optimized synthetic gene encoding residues 13–139 of the SA from *Streptomyces avidinii* into the pET28b expression vector (Novagene, Darmstadt, Germany). Sequence-confirmed SA-ABDwt fusion protein was produced in *E. coli* BL21 λDE3 at 37 °C following IPTG induction (0.5 mM) as insoluble protein into the inclusion bodies [31]. The protein was extracted by solubilisation of washed inclusion bodies with 8 M urea in 50 mM Tris-Cl pH 8 (loading buffer) and the extract was loaded onto DEAE Sepharose column. Upon washing of the resin with 10 bed volumes of the loading buffer, the protein was eluted with 50 mM NaCl in loading buffer. The purified denatured monomeric form of SA-ABDwt was then dialyzed against deionized water buffered to pH 8.5 with ammonia in order to form soluble and stable tetramers, as verified by SDS-PAGE analysis. The final tetrameric form of the SA-ABDwt fusion protein was stored at 4 °C for several days or at −80 °C for several months.

2.5. Data collection and evaluation

The excitation of fluorescence probes and the observation of fluorescence intensity on the surface of the polymeric foil was performed by an inverted optical microscope Olympus IX 71 combined with CoolLED pE 4000 illumination system for fluorescence microscopy. The collected images were cropped and horizontal misalignment was corrected by a freely available version of Zoner Photo Studio 17 software. No other post process steps were performed. The intensity of the fluorescence and of the background signal was evaluated by custom-made scripts written in the sta-

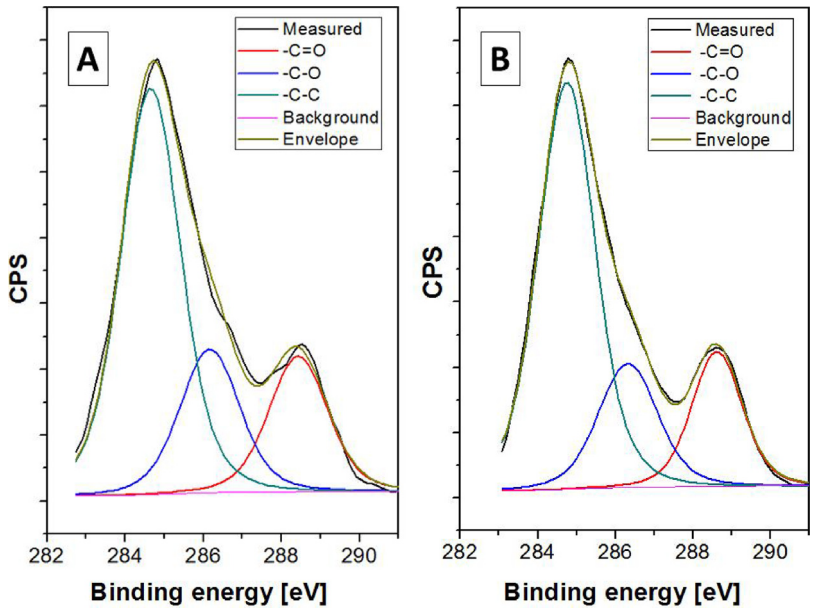

Fig. 2. XPS spectra of the PEN foil surface treated by laser beam.
Detailed carbon C1s XPS spectra of the PEN foil surface treated by laser beam with 8 mJcm^{-2} and 250 (A) or 500 (B) pulses.

tistical language R in RStudio. All data were further processed in statistical software SigmaPlot or GraphPad Prism.

3. Results and discussion

With the aim to design a bioanalytical microsystem for optical affinity-based assays on polymeric PEN foil, we have optimized the fabrication procedure and performed several types of experiments directed to prove, that: i) we are able to covalently graft PEG-biotin molecules onto the PEN foil surface treated with laser beam through a photolithography mask, ii) the number of the pulses of the laser beam can influence the quality of surface modification and biotinylation leading to a lower or a higher signals of the assays, iii) we can perform affinity-based assays of a specific analyte by competitive or direct detection method and detect the specific analyte in the sample, in this particular case, human serum albumin (HSA).

It has been reported that chemical changes on the surface of polymeric materials can be induced by their exposure to high energy radiation such as laser beam [27] or UV radiation [18]. Such processes can be exploited in preparation of biofunctionalized surfaces. In our study, chemical changes on the PEN foil surface were induced by excimer laser beam irradiation of the polymeric foil. The fluence and the number of pulses of the excimer laser beam were optimized before [26,32]. XPS analysis of the PEN foil surface treated with different settings of laser beam is presented in Fig. 2.

The data are in good agreement with our previous studies [26], where we have shown that chemical changes on the surface of PEN foil can be introduced also by irradiation of the foil surface by laser beam through a photolithography mask. Such modified surface can exhibit carbonyl, carboxyl and hydroxyl reactive groups necessary for the subsequent covalent coupling chemistry, as it is obvious from deconvoluted XPS spectra of samples treated with

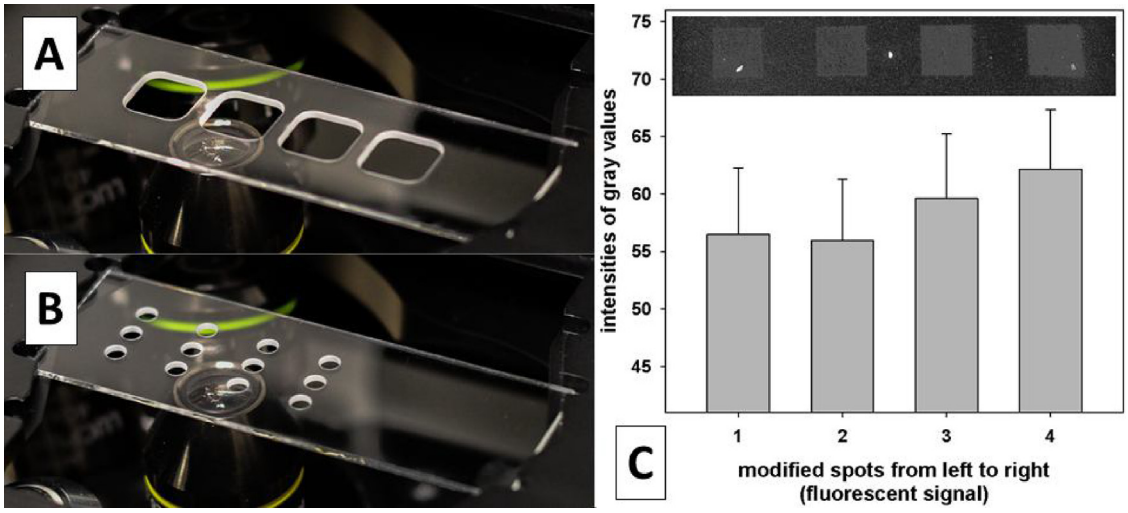

Fig. 3. Fabricated sensing system (data expressed as mean + SD, n = 3).
A well-based sensing system with 4 testing wells (A) and 12 testing wells (B). PEN foil with surface irradiated by laser beam is attached to the bottom side of the glass slide and put on the microscope stage holder. On the bar graph on panel C, we can see the increase in signal intensities of fluorescently labelled streptavidin on biotinylated spots and the corresponding image of the treated spots as inlet. The difference among the spots from the left to the right is caused by irradiation of the PEN foil with uncorrected laser beam through the lithography mask.

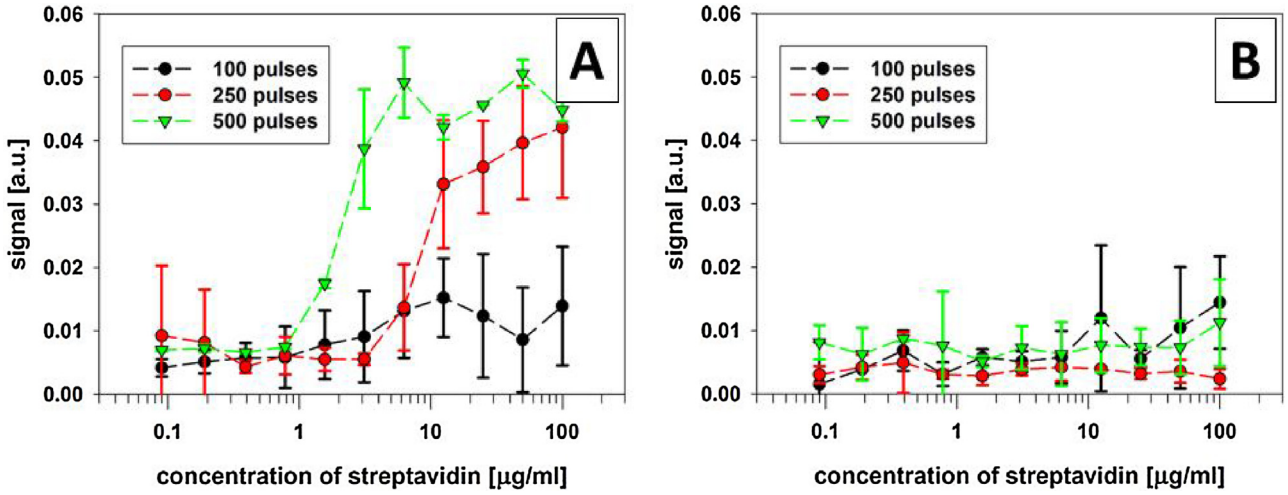

Fig. 4. The signal of the PEN foils treated with different number of laser pulses (data expressed as mean ± SD, n = 6).
The signal of the PEN foil treated with 100, 250 and 500 pulses of laser beam. On panel A, the dependence of signal intensities on the concentration of fluorescently labelled streptavidin is presented. The assays were performed on biotinylated surfaces. On panel B, the same signal intensities are plotted versus different concentrations of fluorescently labelled streptavidin but without the treatment of the foil surface with PEG-biotin (control samples).

8 mJ cm^{-2} and 250 or 500 pulses. The atomic concentration of oxygen was increased with the number of applied laser pulses. We have determined 25.5 ± 0.5% (mean ± SD, n = 3) of oxygen for samples treated with 100 pulses, 27.6 ± 0.8% (mean ± SD, n = 3) for samples treated with 250 pulses, and finally the highest amount of oxygen 28.0 ± 0.8% (mean ± SD, n = 3) was observed for samples treated with 500 pulses. For development of the presented affinity biosensing system, we used EDC coupling chemistry to form amide bonds between amine terminated PEG-biotin and the surface of the PEN foil possessing carboxyl groups generated by laser irradiation.

At the same time, we were creating methodology for fabrication of a well-based format of a sensing system methodology for foil irradiation by laser and for testing samples with a small volume of assay samples. It was important for performing easy and fast measurements of fluorescence intensities with rapid data evaluation. For the purpose of the well-based format of the sensing system and small assay volumes, we cut openings into microscopy glass slides by a microabrasive lathe. The openings were cut into the glass in precisely defined positions corresponding to the micropatterns on the contact mask. Coupling the exposed polymeric foil to the bottom part of the glass slides was performed through transfer adhesive. We optimized the layout of the micropatterns on the contact mask to simplify the process of the foil irradiation just by simple movement of the laser beam above the contact mask, and to increase the number of testing wells on one single slide. At the beginning, the design of the wells on the slide was 1 row with 4 squared wells (the volume of one well was 100–150 µl), Fig. 3A. It was further adjusted into 3 rows with 4 circular wells on one slide (volume of one well was 5–10 µl), Fig. 3B. Because the excimer laser beam has Gaussian fluence profile, the laser beam had to be adjusted for the best fluence distribution in x, y, position [33]. When the beam was not adjusted properly, the irradiated, further modified and analysed spots exhibited an unequal detected signal from the same well, see Fig. 3C.

The final system consisted of 12 testing wells (the optimized sample volume was 8 µl per a well) above the patterned arrays on the PEN foil. It was easy to fabricate and the assays were performed with a very low amount of the sample. The number of wells could be further increased up to 24 wells per one glass slide (substrate 26 × 76 mm) and their size/number was dependent on the arrangement and the size of the laser beam. The measured signal was collected by a camera on an inverted microscope. The process was automated by custom-made scripts actuating microscopy stage and acquiring the pictures. The obtained pictures were manually cropped and the signals from the image data were evaluated automatically by custom-made scripts in program R. With the described workflow, the data collection and the evaluation was semi-automated and very rapid.

The number of the pulses of the laser beam at a given fluence can influence the degree of surface chemical modification, see XPS spectra in Fig. 2. Based on our previous experience and on the published data in [26], the effectivity of laser beam polymer surface modification for coupling chemistry is dependent on the availability of carbonyl reactive groups exposed to the outside of the foil surface and do not only depend on the amount of carbonyl groups detected in the XPS spectra. As a consequence, it can influence the amount of the immobilized biotin on the foil surface and therefore, the intensities of the detected signal during the affinity-based assay performed on the foil. Due to this fact and our previous experience, we micropatterned the foil surface with excimer laser beam with 100, 250 and 500 pulses. PEG-biotin molecules were immobilized on the patterned surface of the foil, and subsequently, the modified surface was incubated with fluorescently labelled streptavidin. Data are presented in Fig. 4.

In Fig. 4A we can see that the maximal intensity of the signal values from samples with 100 pulses is significantly lower comparing to the biotinylated foil surface treated with laser beam with 250 or 500 pulses. The highest signal can be observed and the lowest streptavidin concentrations can be detected with samples treated with 500 pulses comparing to the samples treated with 250 and 100 pulses (Fig. 4A). The signal of the control samples treated with 250 and 500 pulses (Fig. 4B) is significantly lower comparing to the signal of biotinylated foil treated with the same number of pulses. We do not observe great difference between the signal of biotinylated and non-biotinylated samples treated with 100 pulses.

When comparing the images of the detected fluorescent signal from the samples treated with 100, 250 and 500 pulses, we found that the signal on the border of the patterned squares on the samples treated with 500 pulses showed deviations compared to the samples treated with a lower number of laser pulses, see Fig. 5A, B.

Similar behaviour was observed also in our previous studies [26]. When AFM scans were performed in target areas (Fig. 5C, D), the changes in the foil morphology were increasing towards the edges of the patterns, where typical ripples started to have

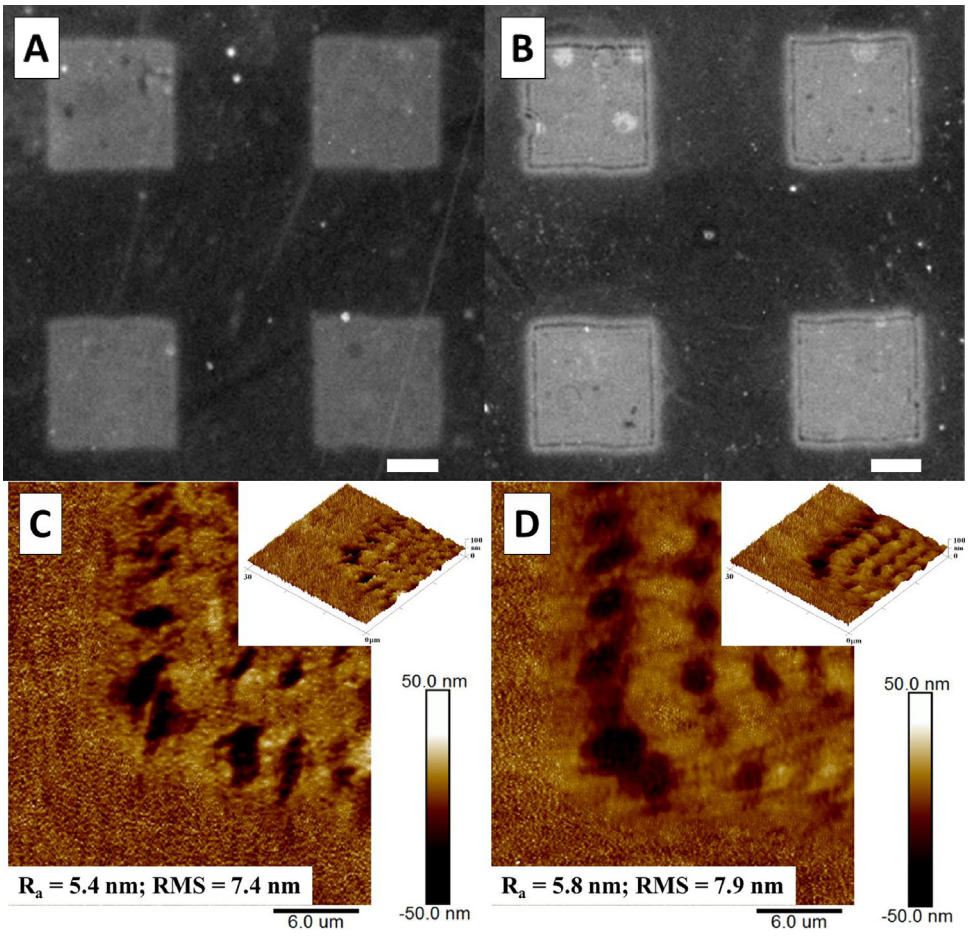

Fig. 5. Influence of laser treatment on the morphology and the signal of the PEN foil.
In the top images (A, B), there is signal of fluorescently labelled streptavidin on biotinylated PEN foil treated by 250 (A) and 500 (B) laser pulses. On panel B we can see deviations of the signal intensities near the borders of the fluorescent spots. In the bottom images (C, D), there are AFM data of the left bottom part of the spots treated by 250 (C) and 500 (D) laser pulses. Deviations of the signal on the spot border (B) correspond to the changes of the surface topology of that place – the hollows on the border. The scale bars on the top panels (A, B) represent 100 μm.

higher amplitude on the patterned surfaces. Similar patterns were also reported in [34], where interference patterns of concentric circles were observed on the PEN foil substrates treated through a glass contact mask with a circular pinhole and also in [35], where a diffraction circular pinhole was used for laser micropatterning of silicon surfaces. Because the morphological changes of the polymer foil treated with laser irradiation with 500 pulses increased and the uniformity of the detected signal on the borders was defected, we decided to micropattern the foil surface only with 250 pulses for further experiments. The described phenomena can be studied in more details in other studies.

When the parameters of the laser treatment were set for the foil micropatterning, we optimized the amount of the immobilized biotin on the surface of the polymer foil in relation to the detected signal of bound, fluorescently labelled, streptavidin. We observed that by increasing the concentrations of the PEG-biotin in the immobilization mixture, the signal of the bound streptavidin increases as well, see Fig. 6A.

Our observation confirms that the amount of the immobilized biotin can significantly influence the detected levels of the measured signal of bound streptavidin, and therefore its immobilized surface density can be further tuned based on the desired application. For any further experiments, we were using the ratio of PEG-biotin in activating buffer 7:1 (concentration of PEG-biotin was 12.5 mg/ml).

To prove that a biotinylated surface of PEN foil is able to selectively bind streptavidin through biotin-streptavidin interactions, we performed competitive assays with a mixture of fluorescently labelled streptavidin (fixed concentration of 25 μg/ml) and non-labelled streptavidin (concentration range 0–100 μg/ml). The data from the assays are presented in Fig. 6B. We can see that both variants of the streptavidin compete for binding to the biotinylated surface and by increasing the concentration of the non-labelled streptavidin, the fluorescent signal decreases. Such behaviour corresponds to the decreased amount of bound fluorescently labelled streptavidin to the biotinylated surface.

After basic characterization of the micropatterned biotinylated surface of the PEN foils discussed above, we performed affinity-based assays with the aim to detect human serum albumin as target model analyte. HSA is one of the most abundant proteins in human plasma, and can be present also in other body fluids such as saliva or urine. It has many functions in the human body and it is also used as biomarker for diagnostic and prognostic purposes in medicine [36]. For the proof-of-concept purpose, we designed a binding assay, based on the recently described SA-ABDwt protein construct [28], which has a natural nM affinity to HSA. It is based on an albumin binding domain (ABD) scaffold of protein G isolated from *Streptococcus* G148, genetically fused with the monomer unit of streptavidin, which spontaneously assembles into tetrameric form. In general, the advantage of using such artificial or genetically modified protein binders comparing to antibodies can be their

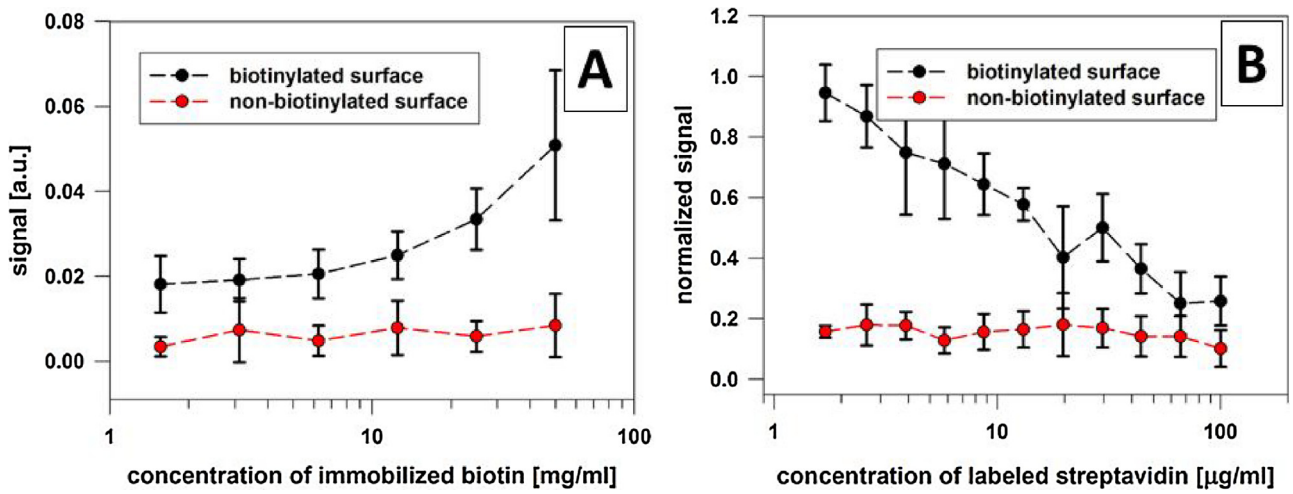

Fig. 6. Optimization of the amount of the immobilized biotin and streptavidin competitive assay (data expressed as mean ± SD, n = 6).
On panel A, the black line represents the signal of fluorescently labelled streptavidin incubated on biotinylated surfaces. It corresponds to the concentration of PEG-biotin molecules in the immobilization mixture. On panel B, the black line represents the signal of fluorescently labelled streptavidin with fixed concentration (25 µg/ml), which competes for binding sites with non-labelled streptavidin. The decrease in the signal intensities of the labelled streptavidin corresponds to the increase in concentration of the non-labelled streptavidin. On both panels, the red line represents control samples, where no biotinylation was performed.

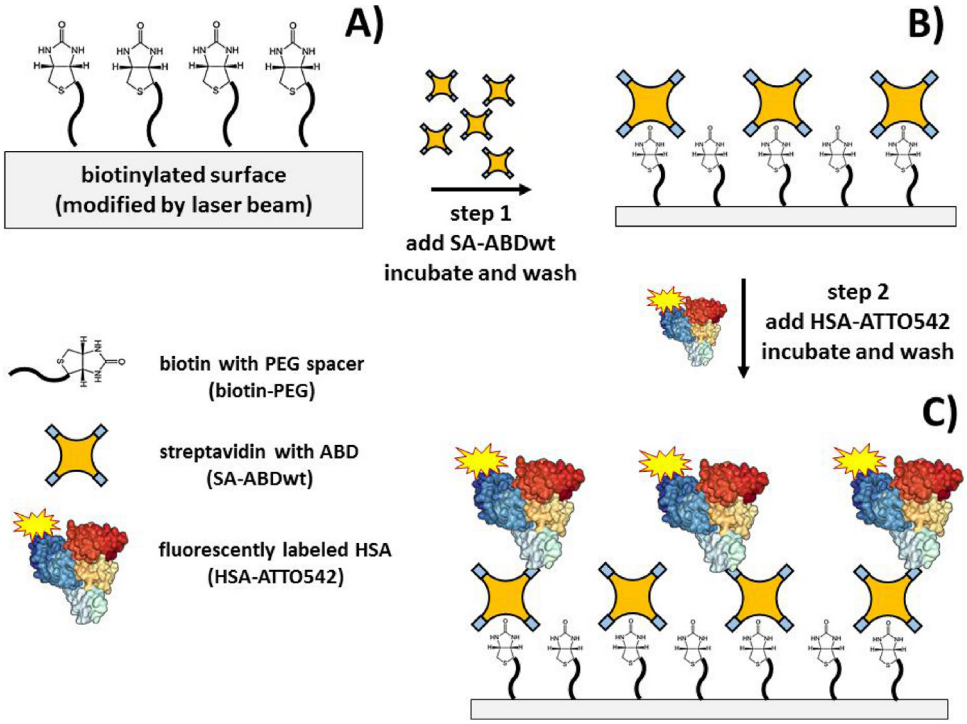

Fig. 7. The principle of the binding assay.
The binding assays were performed on a biotinylated surface of PEN foil (A). In the first step, SA-ABDwt (concentration 10 µg/ml) was incubated with the foil surface and the surface was washed with PBS buffer. It resulted in a specific attachment of the SA-ABDwt to the biotinylated surface (B). In the second step, fluorescently labelled HSA (concentrations 0–30 µg/ml) was incubated with SA-ABDwt on the foil surface and then the surface was washed again with PBS buffer. This step resulted in a specific attachment of the HSA to the foil surface covered with SA-ABDwt (C). Fluorescent detection followed. The pictures of the streptavidin in the presented scheme were generated with the NGL Viewer [38,39].

low molecular weight, simple genetic fusion to other proteins with defined structure and function, possible modifications leading to increased specificity, affinity or stability, and easy and cost-efficient production [37].

The assays were performed in two variants, where i) 1% bovine serum albumin (BSA) and ii) 6% fetal bovine serum (FBS) solutions were used as incubation media. The binding assay on the micro-fabricated PEN foil surface was performed in 2 steps: i) incubation of the biotinylated surface with SA-ABDwt, ii) further incubation of the surface with fluorescently labelled HSA. The principle and details of the binding assays are presented in Fig. 7.

For both assays, calibration binding curves were constructed by fitting the data to the standard sigmoidal curve (software estimated goodness of the fit values were $R^2 = 0.86$ for 1% BSA and $R^2 = 0.94$ for 6% FBS), see Fig. 8. For both types of the experiment, also the limit of detection (LOD) and quantification (LOQ) was calculated as LOD = 1.72 µg/ml and LOQ = 3.09 µg/ml for assays in 1% BSA. For assays in 6% FBS, the obtained values were LOD = 0.09 µg/ml and

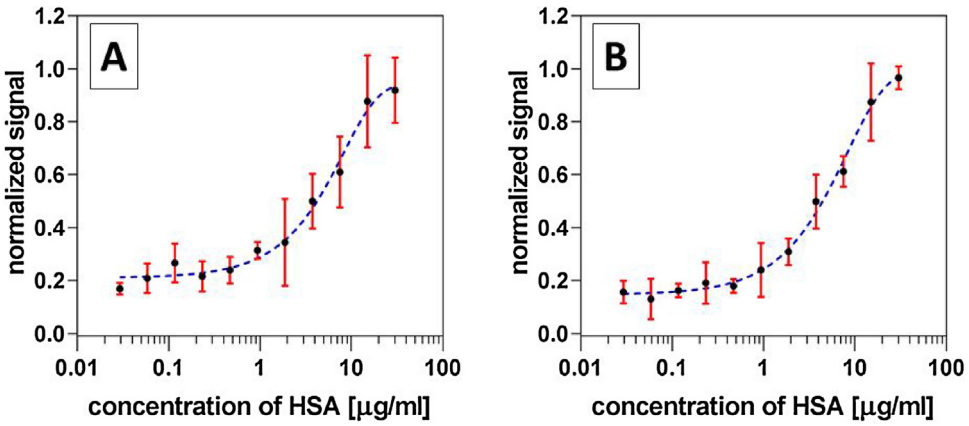

Fig. 8. Affinity-based fluorescent detection of HSA (data expressed as mean ± SD, n = 6).
Affinity-based assays in 1% BSA (A) and in 6% FBS (B) are presented. The blue line represents the sigmoidal fit of the signal of fluorescently labelled HSA specifically bound to the biotinylated surface treated with SA-ABDwt recombinant protein.

LOQ = 2.29 μg/ml. The evaluated limit of detection of HSA in the measured samples was equivalent to ~25.86 nM in 1% BSA and to ~1.35 nM in 6% FBS.

Comparing our calculated LODs for HSA to the other published studies focused on fluorescent immunosensing principles such as detection of HSA in aqueous solution based on time-resolved fluorescence resonance energy transfer [40], detection of HSA on solid support by using quantum dots [41] or to standard ELISA tests [42], our achieved values are higher of one or more orders of magnitude. However, they are comparable or better when compared to other detection methods, for example to commercially available urinalysis test strips [43] or other types of recently published detection methods [44]. Moreover, in general clinical praxis, the detection of serum albumin in association with certain diseases is focused not only on its very low, but also on its high concentrations, depending on its physiological concentration range in body fluids (for example concentration of HSA in saliva ~100–500 μg/ml and urine less then ~4–25 μg/ml [45]).

4. Conclusions

Our work was focused on development of methodology for PEN foil micropatterning by laser beam aimed at designing a sensor with immobilized biotin micropatterns suited for affinity-based optical biosensing. By optimized exposure of PEN foil through a contact lithography mask by laser beam, we achieved chemical changes on the modified polymer, followed by subsequent covalent immobilization of biotin onto its surface. The advantage of the designed process is that it can be developed for high throughput fabrication and roll-to-roll device production.

The modified PEN foil sensing surface was adapted into a well-based format detection system with a low volume of chemical compounds (5–10 μl). As a proof-of-concept, affinity-based fluorescence detection system for human serum albumin (HSA) was tested. Here, a specific binding protein with natural affinity to HSA, the so-called albumin-binding protein domain, genetically fused with streptavidin (SA-ABDwt), was immobilized on the biotinylated surface of the PEN foil. The binding curves between the SA-ABDwt and the fluorescently labelled HSA were measured in different incubation media and conditions, and the calculated LODs were comparable to already published data concerning the detection of HSA. The presented format of the sensing system can be developed into a fully automated fluorescence detection and data evaluation system, and depending on the required HSA detection range, it can be adopted for clinical use.

In conclusion, the presented laser beam micropatterning process enables to produce micropatterned biosensing layers on thin and flexible PEN polymeric material, which can be integrated into simple or more complex sensing devices. The modified surface of polymer can be used for a large range of affinity-based assays, where the overall properties of the sensing system, with respect to the immobilized capture molecules and the type of the target analyte, can be easily optimized. The presented method of polymer surface modification can be further adjusted for other studies and applications.

Acknowledgment

The presented work was supported by the project of Czech Science Foundation (project no. 13-06609S) and with the assistance provided by the Research Infrastructure NanoEnviCz (project no. LM2015073), the project Pro-NanoEnviCz (Reg. no. CZ.02.1.01/0.0/0.0/16_013/0001821), supported by the Ministry of Education, Youth and Sports of the Czech Republic and the European Union – European Structural and Investments Funds in the frame of Operational Programme Research Development and Education and also by the Ministry of Agriculture (project no. QJ1210041).

References

[1] R. Narayanaswamy, O.S. Wolfbeis, Optical Sensors, Springer Berlin Heidelberg, Berlin, Heidelberg, 2004, http://dx.doi.org/10.1007/978-3-662-09111-1.
[2] N.L. Anderson, The clinical plasma proteome: a survey of clinical assays for proteins in plasma and serum, Clin. Chem. 56 (2010) 177–185, http://dx.doi.org/10.1373/clinchem.2009.126706.
[3] P.B. Luppa, L.J. Sokoll, D.W. Chan, Immunosensors—principles and applications to clinical chemistry, Clin. Chim. Acta 314 (2001) 1–26, http://dx.doi.org/10.1016/S0009-8981(01)00629-5.
[4] D. Wild, Immunoassay for beginners, in: Immunoass. Handb., Elsevier, 2013, 2018, pp. 7–10, http://dx.doi.org/10.1016/B978-0-08-097037-0.00002-6.
[5] P.J. Tighe, R.R. Ryder, I. Todd, L.C. Fairclough, ELISA in the multiplex era: potentials and pitfalls, Proteomics – Clin. Appl. 9 (2015) 406–422, http://dx.doi.org/10.1002/prca.201400130.
[6] S.F. Kingsmore, Multiplexed protein measurement: technologies and applications of protein and antibody arrays, Nat. Rev. Drug Discov. 5 (2006) 310–321, http://dx.doi.org/10.1038/nrd2006.
[7] R.P. Ekins, F.W. Chu, Miniaturized microspot multianalyte immunoassay systems, in: Immunoanal. Agrochem, American Chemical Society, 1995, pp. 11–153, http://dx.doi.org/10.1021/bk-1995-0586.ch011.
[8] C.C. Lin, J.H. Wang, H.W. Wu, G. Bin Lee, Microfluidic immunoassays, JALA – J. Assoc. Lab. Autom. 15 (2010) 253–274, http://dx.doi.org/10.1016/j.jala.2010.01.013.
[9] P. Jonkheijm, D. Weinrich, H. Schröder, C.M. Niemeyer, H. Waldmann, Chemical strategies for generating protein biochips, Angew. Chemie – Int. Ed. 47 (2008) 9618–9647, http://dx.doi.org/10.1002/anie.200801711.

[10] V. Romanov, S.N. Davidoff, A.R. Miles, D.W. Grainger, B.K. Gale, B.D. Brooks, A critical comparison of protein microarray fabrication technologies, Analyst 139 (2014) 1303, http://dx.doi.org/10.1039/c3an01577g.
[11] D. Kim, A.E. Herr, Protein immobilization techniques for microfluidic assays, Biomicrofluidics 7 (2013), http://dx.doi.org/10.1063/1.4816934.
[12] M. Focke, D. Kosse, C. Müller, H. Reinecke, R. Zengerle, F. von Stetten, Lab-on-a-Foil: microfluidics on thin and flexible films, Lab Chip 10 (2010) 1365–1386, http://dx.doi.org/10.1039/c001195a.
[13] D. Briand, F. Molina-Lopez, A.V. Quintero, C. Ataman, J. Courbat, N.F. de Rooij, Why going towards plastic and flexible sensors? Procedia Eng. 25 (2011) 8–15, http://dx.doi.org/10.1016/j.proeng.2011.12.004.
[14] T. Velten, H. Schuck, M. Richter, G. Klink, K. Bock, C.K. Malek, S. Roth, H. Schoo, P.J. Bolt, Microfluidics on foil: state of the art and new developments, Proc. Inst. Mech. Eng. Part B J. Eng. Manuf. 222 (2008) 107–116, http://dx.doi.org/10.1243/09544054JEM866.
[15] S. Metz, C. Trautmann, A. Bertsch, P. Renaud, Flexible microchannels with integrated nanoporous membranes for filtration and separation of molecules and particles, Tech. Dig. MEMS 2002 IEEE Int. Conf. Fifteenth IEEE Int. Conf. Micro Electro Mech. Syst. (Cat. No.02CH37266), IEEE (2002) 81–84, http://dx.doi.org/10.1109/MEMSYS.2002.984095.
[16] J. Gamby, M. Lazerges, H.H. Girault, C. Deslouis, C. Gabrielli, H. Perrot, B. Tribollet, Electroacoustic polymer microchip as an alternative to quartz crystal microbalance for biosensor development, Anal. Chem. 80 (2008) 8900–8907, http://dx.doi.org/10.1021/ac800443u.
[17] B. Rubehn, C. Bosman, R. Oostenveld, P. Fries, T. Stieglitz, A MEMS-based flexible multichannel ECoG-electrode array, J. Neural Eng. 6 (2009) 36003, http://dx.doi.org/10.1088/1741-2560/6/3/036003.
[18] J.M. Goddard, J.H. Hotchkiss, Polymer surface modification for the attachment of bioactive compounds, Prog. Polym. Sci. 32 (2007) 698–725, http://dx.doi.org/10.1016/j.progpolymsci.2007.04.002.
[19] H. Becker, U. Heim, Hot embossing as a method for the fabrication of polymer high aspect ratio structures, Sens. Actuators A Phys. 83 (2000) 130–135, http://dx.doi.org/10.1016/S0924-4247(00)00296-X.
[20] B. Feyssa, C. Liedert, L. Kivimaki, L.-S. Johansson, H. Jantunen, L. Hakalahti, Patterned immobilization of antibodies within roll-to-roll hot embossed polymeric microfluidic channels, PLoS One 8 (2013) e68918, http://dx.doi.org/10.1371/journal.pone.0068918.
[21] J. Dutta Majumdar, I. Manna, Laser material processing, Int. Mater. Rev. 56 (2011) 341–388, http://dx.doi.org/10.1179/1743280411Y.0000000003.
[22] M. Castillejo, T.A. Ezquerra, M. Martín, M. Oujja, S. Pérez, E. Rebollar, Laser Nanostructuring of Polymers: Ripples and Applications, 2012, pp. 372–380, http://dx.doi.org/10.1063/1.4739891.
[23] P. Slepička, A. Chaloupka, P. Sajdl, J. Heitz, V. Hnatowicz, V. Švorčík, Angle dependent laser nanopatterning of poly(ethylene terephthalate) surfaces, Appl. Surf. Sci. 257 (2011) 6021–6025, http://dx.doi.org/10.1016/j.apsusc.2011.01.107.
[24] P. Slepička, I. Michaljaničová, S. Rimpelová, V. Švorčík, Surface roughness in action - cells in opposition, Mater. Sci. Eng. C 76 (2017) 818–826, http://dx.doi.org/10.1016/j.msec.2017.03.061.
[25] P. Slepička, I. Michaljaničová, P. Sajdl, P. Fitl, V. Švorčík, Surface ablation of PLLA induced by KrF excimer laser, Appl. Surf. Sci. 283 (2013) 438–444, http://dx.doi.org/10.1016/j.apsusc.2013.06.127.
[26] M. Štofik, A. Semerádtová, J. Malý, Z. Kolská, O. Neděla, D. Wrobel, P. Slepička, Direct immobilization of biotin on the micro-patterned PEN foil treated by excimer laser, Colloids Surf. B Biointerfaces 128 (2015) 363–369, http://dx.doi.org/10.1016/j.colsurfb.2015.02.032.
[27] O. Neděla, P. Slepička, J. Malý, M. Štofík, V. Švorčík, Laser-induced nanostructures on a polymer irradiated through a contact mask, Appl. Surf. Sci. 321 (2014) 173–178, http://dx.doi.org/10.1016/j.apsusc.2014.09.187.
[28] J. Maly, O. Stanek, J. Frolik, M. Maly, F. Ennen, D. Appelhans, A. Semeradtova, D. Wrobel, M. Stofik, T. Knapova, M. Kuchar, L.C. Stastna, J. Cermak, P. Sebo, P. Maly, Biocompatible size-defined dendrimer-albumin binding protein hybrid materials as a versatile platform for biomedical applications, Macromol. Biosci. 16 (2016) 553–566, http://dx.doi.org/10.1002/mabi.201500332.
[29] T. Peterbauer, J. Heitz, M. Olbrich, S. Hering, Simple and versatile methods for the fabrication of arrays of live mammalian cells, Lab Chip 6 (2006) 857, http://dx.doi.org/10.1039/b601803c.
[30] J.N. Ahmad, J. Li, L. Biedermannová, M. Kuchař, H. Šípová, A. Semerádtová, J. Černý, H. Petroková, P. Mikulecký, J. Polínek, O. Staněk, J. Vondrášek, J. Homola, J. Malý, R. Osička, P. Šebo, P. Malý, Novel high-affinity binders of human interferon gamma derived from albumin-binding domain of protein G, Proteins Struct. Funct. Bioinf. 80 (2012) 774–789, http://dx.doi.org/10.1002/prot.23234.
[31] C. Bernelin-Cottet, C. Deloizy, O. Stanek, C. Barc, E. Bouguyon, C. Urien, O. Boulesteix, J. Pezant, C.-A. Richard, M. Moudjou, B. Da Costa, L. Jouneau, C. Chevalier, C. Leclerc, P. Sebo, N. Bertho, I. Schwartz-Cornil, Corrigendum a universal influenza vaccine can lead to disease exacerbation or viral control depending on delivery strategies, Front. Immunol. 8 (2017) 831, http://dx.doi.org/10.3389/fimmu.2017.00831.
[32] P. Slepička, O. Neděla, P. Sajdl, Z. Kolská, V. Švorčík, Polyethylene naphthalate as an excellent candidate for ripple nanopatterning, Appl. Surf. Sci. 285 (2013) 885–892, http://dx.doi.org/10.1016/j.apsusc.2013.09.007.
[33] J. Kruger, W. Kautek, Ultrashort pulse laser interaction with dielectrics and polymers, Adv. Polym. Sci. 168 (2004) 247–289, http://dx.doi.org/10.1007/B12683.
[34] O. Neděla, P. Slepička, P. Sajdl, M. Veselý, V. Švorčík, Surface analysis of ripple pattern on PS and PEN induced with ring-shaped mask due to KrF laser treatment, Surf. Interface Anal. 49 (2017) 25–33, http://dx.doi.org/10.1002/sia.6054.
[35] E. Haro-Poniatowski, C. Acosta-Zepeda, G. Mecalco, J.L. Hernández-Pozos, N. Batina, I. Morales-Reyes, J. Bonse, Diffraction-assisted micropatterning of silicon surfaces by ns-laser irradiation, J. Appl. Phys. 115 (2014) 13–19, http://dx.doi.org/10.1063/1.4882660.
[36] G.J. Quinlan, G.S. Martin, T.W. Evans, Albumin Biochemical properties and therapeutic potential, Hepatology 41 (2005) 1211–1219, http://dx.doi.org/10.1002/hep.20720.
[37] T. Hey, E. Fiedler, R. Rudolph, M. Fiedler, Artificial, non-antibody binding proteins for pharmaceutical and industrial applications, Trends Biotechnol. 23 (2005) 514–522, http://dx.doi.org/10.1016/j.tibtech.2005.07.007.
[38] A.S. Rose, A.R. Bradley, Y. Valasatava, J.M. Duarte, A. Prlić, P.W. Rose, Web-based molecular graphics for large complexes, in: Proc. 21 st Int. Conf. Web3D Technol. – Web3D '16, ACM Press, New York, New York, USA, 2016, pp. 185–186, http://dx.doi.org/10.1145/2945292.2945324.
[39] A.S. Rose, P.W. Hildebrand, NGL Viewer: a web application for molecular visualization, Nucleic Acids Res. 43 (2015) W576–W579, http://dx.doi.org/10.1093/nar/gkv402.
[40] R.E. Wang, L. Tian, Y.-H. Chang, A homogeneous fluorescent sensor for human serum albumin, J. Pharm. Biomed. Anal. 63 (2012) 165–169, http://dx.doi.org/10.1016/j.jpba.2011.12.035.
[41] M.-C. Tu, Y.-T. Chang, Y.-T. Kang, H.-Y. Chang, P. Chang, T.-R. Yew, A quantum dot-based optical immunosensor for human serum albumin detection, Biosens. Bioelectron. 34 (2012) 286–290, http://dx.doi.org/10.1016/j.bios.2011.11.035.
[42] S. Akman, I. Kurt, M. Gultepe, I. Dibirdik, C. Kilinc, T. Kutluay, L. Karaca, N.K. Bingol, The development and validation of a competitive, microtiter plate enzymeimmunoassay for human albumin in urine, J. Immunoassay 16 (1995) 279–296, http://dx.doi.org/10.1080/15321819508013563.
[43] J. Penders, T. Fiers, J.R. Delanghe, Quantitative evaluation of urinalysis test strips, Clin. Chem. 48 (2002) 2236–2241 http://www.ncbi.nlm.nih.gov/pubmed/12446482.
[44] A.F. Ogata, J.M. Edgar, S. Majumdar, J.S. Briggs, S.V. Patterson, M.X. Tan, S.T. Kudlacek, C.A. Schneider, G.A. Weiss, R.M. Penner, Virus-enabled biosensor for human serum albumin, Anal. Chem. 89 (2017) 1373–1381, http://dx.doi.org/10.1021/acs.analchem.6b04840.
[45] T. Peters Jr., All about albumin, in: Biochemistry, Genetics, and Medical Applications, Academic Press, San Diego, 1995.